ЖЭТФ, 2014, том 145, вып. 5, стр. 877–891

ZONE STRUCTURE AND POLARIZATION PROPERTIES OF THE STACK OF A METAMATERIAL-BASED CHOLESTERIC LIQUID CRYSTAL AND ISOTROPIC MEDIUM LAYERS

A. H. Gevorgyan[a]*, *G. K. Matinyan*[b]

[a] *Department of Physics, Yerevan State University*
0025, Yerevan, Armenia

[b] *Armenian Agrarian State University*
009, Yerevan, Armenia

Received May 26, 2013

The optical properties of a stack of metamaterial-based cholesteric liquid crystal (CLC) layers and isotropic medium layers are investigated. The problem is solved by a modification of Ambartsumian's layer addition method. CLCs with two types of chiral nihility are defined. The peculiarities of the reflection spectra of this system are investigated and it is shown that the reflection spectra of the stacks of CLC layers of these two types differ from each other. Besides, in contrast to the single CLC layer case, these systems have multiple photonic band gaps. There are two types of such gaps: those selective with respect to polarization of the incident light and nonselective ones. It is shown that the system eigenpolarizations mainly coincide with the quasi-orthogonal, quasi-circular polarizations for normally incident light, except the regions of diffraction reflection selective with respect to the polarization of incident light. The influence of the CLC sublayer thicknesses, the incidence angle, the local dielectric (magnetic) anisotropy of the CLC layers, and the refractive indices and thicknesses of the isotropic media layers on the reflection spectra and other optical characteristics of the system is investigated.

DOI: 10.7868/S0044451014050115

1. INTRODUCTION

Material science was energetically developing recently, and its part concerning the optical materials was developing even more energetically. In particular, metamaterials are of great interest. Metamaterials are artificial composites containing sublongwave structures and exhibiting new linear and nonlinear optical properties such as negative refraction, reverse Doppler effect, electromagnetic energy propagation in the direction opposite to the wave vector, and so on [1–9]. They have surprising applications to perfect lenses [10], invisible cloaks [11–16], perfect absorbers [17], etc.

Investigations of photonic crystals (PCs) are still of great interest both for their wide application in science and techniques and for developing the modern technology of creating new media. They have a photonic band gap (PBG) in their transmittance spectrum that can be changed either by external fields or by the changes in the crystal internal structure [18–20]. The optical devices based on PCs have such properties as multifunctionality and tunability, compactness and low energetic losses, high reliability and good compatibility with other optical devices. Cholesteric liquid crystals (CLCs) are known as PCs with easily tunable parameters (their parameters can be tuned by external electric, magnetic, and strong light fields, thermal gradients, or UV radiation, etc.) A CLC is a self-assembled PC formed by rod-like molecules, including chiral molecules that arrange themselves in a helical fashion. The CLC has a single PBG and an associated one-color reflection band for circularly polarized light with the same handedness as the CLC helix (at normal light incidence). On the other hand, PCs with multiple (polychromatic) PBGs are attracting much attention recently. They find wide application, in particular, in display industry.

Multiple PBGs of one-dimensional structures containing CLC and isotropic layers were reported in some theoretical and experimental works [21–23]. Analoguos investigations of one-dimensional multilayer structures

*E-mail: agevorgyan@ysu.am

containing CLC and anisotropic layers were carried out in [24]. In [25], quasi-periodic systems described by the Fibonacci sequence and containing CLC layers were investigated. The multiple PBGs are also formed in a stack containing right- and left-hand CLC layers [26–30]. In [31], the reflection and polarization peculiarities of stacks of CLC and isotropic media layers were investigated.

Recently, the chiral nihility media have become interesting. The concept of chiral nihility in electromagnetism was introduced by Lakhtakia [32], as a medium in which both dielectric and magnetic permittivities are zero. The nihility concept was then applied to isotropic chiral metamaterials in [33], whose peculiarities have recently been energetically investigated in [34–37] (also see the references in them).

In this paper the concept of nihility is generalized to structurally chiral media (such as CLC) and, using it, the peculiarities of a stack formed by CLC layers with nihility and isotropic media layers are investigated.

2. THE METHOD OF ANALYSIS

The problem is solved by a modification of Ambartsumian's layer addition method [26, 38]. According to [26, 38], if there is a system containing two layers, A and B, stacked up "from left to right", then the reflection and transmission matrices of the system A+B, denoted by $\hat{R}_{A+B}$ and $\hat{T}_{A+B}$, are defined by the analogous matrices of the separate layers as follows:

$$\begin{aligned} \hat{R}_{A+B} &= \hat{R}_A + \tilde{\hat{T}}_A \hat{R}_B \left[\hat{I} - \tilde{\hat{R}}_A \hat{R}_B\right]^{-1} \hat{T}_A, \\ \hat{T}_{A+B} &= \hat{T}_B \left[\hat{I} - \tilde{\hat{R}}_A \hat{R}_B\right]^{-1} \hat{T}_A, \end{aligned} \tag{1}$$

where $\hat{I}$ is the unit matrix and the tilde denotes the reflection and transmission matrices of the reverse light propagation. The same matrices for the reverse propagation of light are defined by the matrix equations

$$\begin{aligned} \tilde{\hat{R}}_{A+B} &= \tilde{\hat{R}}_B + \hat{T}_B \tilde{\hat{R}}_A \left[\hat{I} - \hat{R}_B \tilde{\hat{R}}_A\right]^{-1} \tilde{\hat{T}}_B, \\ \tilde{\hat{T}}_{A+B} &= \tilde{\hat{T}}_A \left[\hat{I} - \hat{R}_B \tilde{\hat{R}}_A\right]^{-1} \tilde{\hat{T}}_B. \end{aligned} \tag{2}$$

In the case where the subject layer borders the same medium on its both sides, the reflection and transmission matrices for the incidence "from right to left" are related by

$$\tilde{\hat{T}} = \hat{F}^{-1} \hat{T} \hat{F}, \quad \tilde{\hat{R}} = \hat{F}^{-1} \hat{R} \hat{F}, \tag{3}$$

where $\hat{F} = \begin{pmatrix} 1 & 0 \\ 0 & -1 \end{pmatrix}$ for linear base polarizations and $\hat{F} = \begin{pmatrix} 0 & 1 \\ 1 & 0 \end{pmatrix}$ for circular base polarizations. The exact reflection and transmission matrices for a finite CLC layer (for normal light incidence) and an isotropic layer of a finite thickness are well known [39, 40].

Transmission/reflection through a stack of CLC layers and isotropic medium layers is calculated using matrix equations (1) by successively applying them to the new layers added to the stack; the stack was considered as layer A and the added layer as layer B. Hence, to organize the calculations more conveniently, system (1) is presented in the form of difference matrix equations

$$\begin{aligned} \hat{R}_j &= \hat{r}_j + \tilde{\hat{t}}_j \hat{R}_{j-1} \left(\hat{I} - \tilde{\hat{r}}_j \hat{R}_{j-1}\right)^{-1} \hat{t}_j, \\ \hat{T}_j &= \hat{T}_{j-1} \left(\hat{I} - \tilde{\hat{r}}_j \hat{R}_{j-1}\right)^{-1} \hat{t}_j \end{aligned} \tag{4}$$

with $\hat{R}_0 = \hat{0}$ and $\hat{T}_0 = \hat{I}$. Here, $\hat{R}_j$, $\hat{T}_j$, $\hat{R}_{j-1}$, and $\hat{T}_{j-1}$ are the reflection and transmission matrices for the systems with j and $j-1$ sublayers respectively, and $\hat{r}_j$ and $\hat{t}_j$ are the reflection and transmission matrices for the jth sublayer and $\hat{0}$ is the zero matrix.

It is to be noted that in [41, 42], a new method for solving the problem of light propagation through a one-dimensional layer system was described.

We now pass to the eigenpolarizations (EPs) and eigenvalues of the amplitude. As is known, EPs are the two polarizations of the incident wave that do not change when passed through the system, and the eigenvalues are the amplitude coefficients of reflection and transmission for the incident light with the EPs [38, 40]. The EPs and eigenvalues deliver much information about the interaction of light with the system; therefore, their calculation is important for every optical system. It follows from the definition of EPs that they must be connected with the polarizations of the internal waves (eigenmodes) excited in the medium (they mainly coincide with the polarizations of eigenmodes). Our investigations show, in particular, that in homogeneous media and CLC (for the normal incidence) for which the exact solution is known and hence the polarizations of the eigenmodes are known, the EPs practically coincide with the polarizations of eigenmodes. As is known (in particular, for normal incidence), the EPs of CLCs or gyrotropic media practically coincide with the orthogonal circular polarizations, whereas for nongyrotropic media, they coincide with the orthogonal linear polarizations. It follows from the foregoing that the investigation of the EP peculiarities is especially important in the case of nonhomogeneous media, for which, in general, the exact solution of the problem is not known.

We let the ratio of the field complex amplitude components at the entrance of the system be denoted by χ_i ($\chi_i = E_i^s/E_i^p$) and that at the exit of the system by χ_t ($\chi_t = E_t^s/E_t^p$), and take into account that

$$\begin{bmatrix} E_t^p \\ E_t^s \end{bmatrix} = \begin{bmatrix} T_{11} & T_{12} \\ T_{21} & T_{22} \end{bmatrix} \begin{bmatrix} E_i^p \\ E_i^s \end{bmatrix}$$

to obtain their relation:

$$\chi_t = \frac{T_{22}\chi_i + T_{21}}{T_{12}\chi_i + T_{11}}. \quad (5)$$

The function, $\chi_t = f(\chi_i)$, is called the polarization transfer function [40]; it carries information about the transformation of the polarization ellipse as light passes through the system. Every optical system has two EPs obtained from the definition of EPs: $\chi_i = \chi_t$. Hence, according to (5), the χ_1 and χ_2 EPs are given by

$$\chi_{1,2} = \frac{T_{22} - T_{11} \pm \sqrt{(T_{22} - T_{11})^2 + 4T_{12}T_{21}}}{2T_{12}}. \quad (6)$$

The ellipticity $e_{1,2}$ and the azimuth $\psi_{1,2}$ of the EPs are expressed in terms of $\chi_{1,2}$ as

$$\begin{gathered} \psi_{1,2} = \frac{1}{2} \operatorname{arctg} \frac{2\chi_{1,2}}{1 - |\chi_{1,2}|^2}, \\ e_{1,2} = \operatorname{tg}\left(\frac{1}{2} \arcsin \frac{2\operatorname{Im}\chi}{1 + |\chi|^2}\right). \end{gathered} \quad (7)$$

3. RESULTS AND DISCUSSION

Now we analyze the spectra peculiarities of the multilayer structure that is a stack of CLC layers with nihility and an isotropic medium layers (Fig. 1). We first discuss some properties of a single CLC layer and the possibility of generalizing the chiral nihility concept for CLCs. We assume that the electromagnetic wavelength is longer than the characteristic lengths of the subject metamaterial structure elements (of which the medium is composed), which allows considering the medium continuous and characterizing it in terms of the dielectric and magnetic permittivity matrices of the form

$$\begin{gathered} \hat{\varepsilon}(z) = \begin{pmatrix} \varepsilon_m + \dfrac{\Delta\varepsilon}{2}\cos(2az) & \dfrac{\Delta\varepsilon}{2}\sin(2az) & 0 \\ \dfrac{\Delta\varepsilon}{2}\sin(2az) & \varepsilon_m - \dfrac{\Delta\varepsilon}{2}\cos(2az) & 0 \\ 0 & 0 & \varepsilon_2 \end{pmatrix}, \\ \hat{\mu}(z) = \begin{pmatrix} \mu_m + \dfrac{\Delta\mu}{2}\cos(2az) & \dfrac{\Delta\mu}{2}\sin(2az) & 0 \\ \dfrac{\Delta\mu}{2}\sin(2az) & \mu_m - \dfrac{\Delta\mu}{2}\cos(2az) & 0 \\ 0 & 0 & \mu_2 \end{pmatrix}, \end{gathered} \quad (8)$$

where

$$\varepsilon_m = \frac{\varepsilon_1 + \varepsilon_2}{2}, \quad \mu_m = \frac{\mu_1 + \mu_2}{2},$$

$$\Delta\varepsilon = \frac{\varepsilon_1 - \varepsilon_2}{2}, \quad \Delta\mu = \frac{\mu_1 - \mu_2}{2},$$

ε_1 and ε_2 are the principal values of the dielectric tensor, μ_1 and μ_2 are those of the magnetic tensor, and $a = 2\pi/p$, where p is the helix pitch.

It is known (see, e. g., [43, 44]) that the solutions of Maxwell's equations (for normal light incidence) for the CLC with the dielectric and magnetic tensors given by (8) have the form

$$\mathbf{E}(z,t) = \sum_{j=1}^{4} \left[E_j^+ \mathbf{n}_+ \exp(ik_j^+ z) + E_j^- \mathbf{n}_- \exp(ik_j^- z)\right] \times \exp(-i\omega t). \quad (9)$$

Here, $\mathbf{n}_\pm = (\mathbf{e}_x \pm i\mathbf{e}_y)/\sqrt{2}$ are the circular polarization unit vectors, ω is the light frequency in the vacuum, and k_j^+ and k_j^- are the z components of the wave vectors ($k_j^+ - k_j^- = 2a$) that are defined from the dispersion equation and have following form

$$k_j^+ = a \pm K_{1,2}, \quad k_j^- = -a \pm K_{1,2}, \quad j = 1,2,3,4, \quad (10)$$

where

$$K_{1,2} = \left\{ \frac{\omega^2}{c^2} \frac{\varepsilon_1\mu_2 + \varepsilon_2\mu_1}{2} + a^2 \pm \right.$$

$$\left. \pm \left[\left(\frac{\omega^2}{c^2} \frac{\varepsilon_1\mu_2 - \varepsilon_2\mu_1}{2} \right)^2 + 4a^2 \frac{\omega^2}{c^2} \varepsilon_m \mu_m \right]^{1/2} \right\}^{1/2}. \quad (11)$$

The amplitudes E_j^+ and E_j^- are related as

$$\xi_j = \frac{E_j^-}{E_j^+} = \frac{1 - i\tau_j}{1 + i\tau_j}, \quad (12)$$

where

$$\tau_{1,2} = \frac{iaK_{1,2}(\mu_1 + \mu_2)}{K_{1,2}^2 \mu_2 + a^2 \mu_1 - (\omega^2/c^2)\mu_1\mu_2\varepsilon_2}.$$

In the investigations of optical properties of CLCs, two coordinate frames are commonly used: the laboratory frame (x, y, z), with the z axis parallel to the axis of the CLC helix, and the rotating frame (x', y', z'), with the z' axis coinciding with the z axis, and the x' and y' axes being parallel to the primary direction of the dielectric permittivity (magnetic permeability) tensor. Two approaches are possible when solving Maxwell's equations [45].

1) Leaving the vectors of the electric and magnetic fields as well as the two corresponding inductions invariable, we can transform the tensor of the dielectric permittivity to the form

$$\hat{\varepsilon}(z) = \hat{R}(az)\hat{\varepsilon}_0 R^{-1}(az),$$

where

$$\hat{\varepsilon}_0 = \begin{pmatrix} \varepsilon_1 & 0 & 0 \\ 0 & \varepsilon_2 & 0 \\ 0 & 0 & \varepsilon_2 \end{pmatrix}$$

is the dielectric permittivity local tensor, and the rotation matrix is

$$\hat{R}(az) = \begin{pmatrix} \cos(az) & -\sin(az) & 0 \\ \sin(az) & \cos(az) & 0 \\ 0 & 0 & 1 \end{pmatrix}$$

(and the same for the magnetic permeability).

2) Leaving the dielectric permittivity tensor (and the magnetic permeability tensor) invariable in the local rotating frame, we can transform the vectors of electric/magnetic fields and the corresponding inductions according to the equation $\mathbf{E}(z) = \hat{R}^{-1}(az)\vec{\mathcal{E}}(z)$.

Both methods are equivalent and ultimately give the same result. Formula (9) is the solution of Maxwell's equation in the laboratory frame. We only note that the solution of Maxwell's equations in the rotating frame has the form

$$\vec{\mathcal{E}}(z,t) = \sum_{j=1}^{4} \vec{\mathcal{E}}_{0j} \exp(iK_j z) \exp(-i\omega t), \quad (13)$$

i. e., K_j are the wave vectors of the fields in the rotating frame. Thus, (9) is the solution of Maxwell's equations in the laboratory frame and (13) is that in the rotating frame and, accordingly, $k_j^{\pm}$ $(j = 1, 2, 3, 4)$ are the wave numbers in the laboratory frame and $\pm K_{1,2}$ are those in the rotating frame.

Figure 2 presents the dependences of $K_{1,2}$ on the wavelength for the CLC with low dielectric and magnetic anisotropies. From the four roots only those two are selected that have positive imaginary parts. It follows from (9) that for light propagation along the medium axis, only four eigenmodes are present, each of which is a superposition of two circularly polarized plane waves. According to the signs of k_j^+ and k_j^- in formula (9), they can be either two waves with opposite circular polarizations traveling in the same direction (in the case of the same signs of k_j^+ and k_j^-) or two waves with the same circular polarization traveling in the opposite directions (in the case of the opposite signs of k_j^+ and k_j^-). As can be seen from the figure, there is a wavelength region where $K_{1,2}$ are purely imaginary. This wavelength region corresponds to the PBG, that is, the propagating waves polarized circularly and having the same handedness as the media helix are absent in this region. We have $|\xi_2| = 1$ in the PBG. The PBG borders are defined from the condition $K_2 = 0$ and have the forms

$$\lambda_1 = p\sqrt{\varepsilon_1\mu_1}, \quad \lambda_2 = p\sqrt{\varepsilon_2\mu_2}. \quad (14)$$

We note again that only the eigenmode with the circular polarization coincident with the CLC helix handedness undergoes diffraction reflection, in the case of light propagation along the CLC axis and for low local anisotropy. Substantially, the diffraction reflection takes place only in the first order and it is completely absent in all higher orders, which is illustrated by the dispersion curves in Fig. 2.

The peculiarities of the eigensolutions of CLCs are investigated in [46] and the possibilities of exciting new types of PBGs are presented for large anisotropies of the medium, namely, the direct and the indirect nonselective PBGs (with respect to the incident light polarizations, in contrast to the usual PBGs, which are selective with respect to the polarization of incident light).

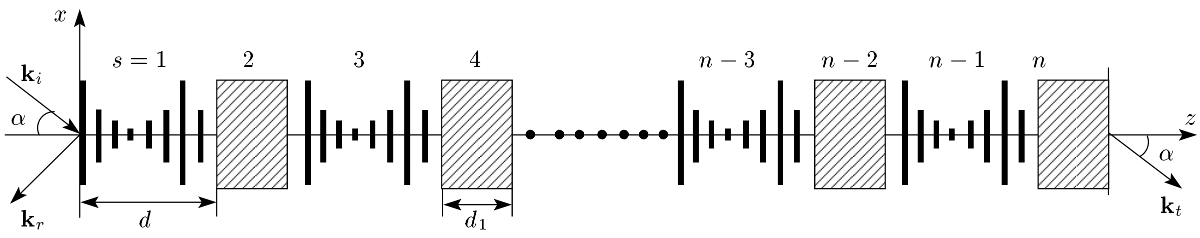

Fig. 1. Sketch of a stack of CLC layers and isotropic medium layers

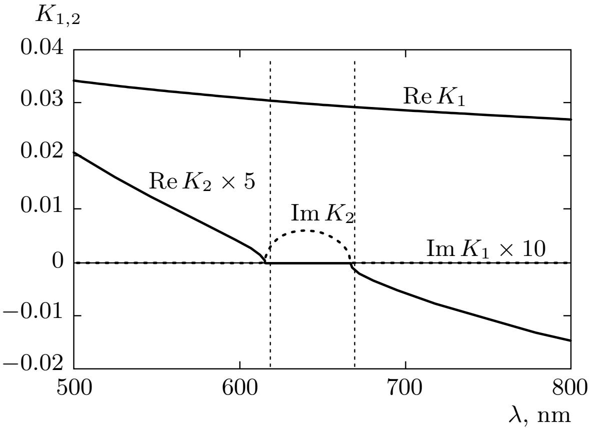

Fig. 2. The dependences of $K_{1,2}$ on the wavelength λ. The CLC parameters are $\varepsilon_1 = 2.29$, $\varepsilon_2 = 2.143$, $\mu_1 = 1.1$, $\mu_2 = 1$, and $p = 420$ nm

As is well known [33], the isotropic chiral nihility metamaterials are the media with the parameters $\varepsilon = 0$, $\mu = 0$, and $\rho \neq 0$ (here, ρ is the chirality parameter of the isotropic chiral metamaterial). Because a CLC is locally anisotropic, we define the CLC with chiral nihility as the CLC with $\varepsilon_m = \mu_m = 0$ and $p \neq 0$. There can be two types of helicoidal structures with such parameters

1) $\varepsilon_1/\mu_1 = \varepsilon_2/\mu_2 < 0$ (chiral nihility of the first type);

2) $\varepsilon_1/\mu_1 = \varepsilon_2/\mu_2 > 0$ (chiral nihility of the second type).

Both types differ from each other only by the phase of the modulation of dielectric and magnetic permittivities; in the first case, these phases coincide, and in the second case, the phase difference is $\pi/2$.

For these conditions, we have

$$\sqrt{\left(\frac{\omega^2}{c^2}\,\frac{\varepsilon_1\mu_2 - \varepsilon_2\mu_1}{2}\right)^2 + 4a^2\frac{\omega^2}{c^2}\,\varepsilon_m\mu_m} = 0,$$

$$K_{1,2} = \sqrt{\frac{\omega^2}{c^2}\,\frac{\varepsilon_1\mu_2 + \varepsilon_2\mu_1}{2} + a^2}.$$

In the first case,

$$\frac{\omega^2}{c^2}\,\frac{\varepsilon_1\mu_2 + \varepsilon_2\mu_1}{2} + a^2 > 0,$$

and therefore $K_{1,2}$ are always real (of course, in the absence of absorption or amplification), whereas in the second case, the values of $K_{1,2}$ are purely imaginary at the wavelengths

$$\lambda \leq p\sqrt{\left|\frac{\varepsilon_1\mu_2 + \varepsilon_2\mu_1}{2}\right|}. \qquad (15)$$

According to these formulas, in the first case, the CLC layer is transparent, and in the second case, a PBG of a new type appears in the spectrum region (15) defined above, where the CLC completely reflects the incidence light with any polarization.

In Fig. 3, the dependences of the wave numbers $K_{1,2}$ on the wavelength for the CLCs of the above two types of chiral nihility are presented.

We now pass to the investigation of the peculiarities of the reflection spectra, polarization plane rotation, and the azimuth and ellipticity of the EPs of a stack composed of CLC layers and isotropic medium layers.

3.1. Reflection spectra. Spectra of the polarization characteristics

We first note once again that the optical property peculiarities of a stack composed of CLC and isotropic medium layers at low dielectric and magnetic anisotropies of CLC layers were discussed in [31]. In Fig. 4, we show the reflection spectra, the polarization plane rotation and the polarization ellipticity spectra, and the spectra of the azimuth and the ellipticity of the first EP for normal light incidence in cases when the CLC layers in the stack have chiral nihility of the first and second type. In Figs. 4*a* and 4*b*, the incident light has the right (solid curve) and left (dashed curve) circular polarizations; in Fig. 4*c*,*d*, it has linear polarization along the x axis. The CLC helices are

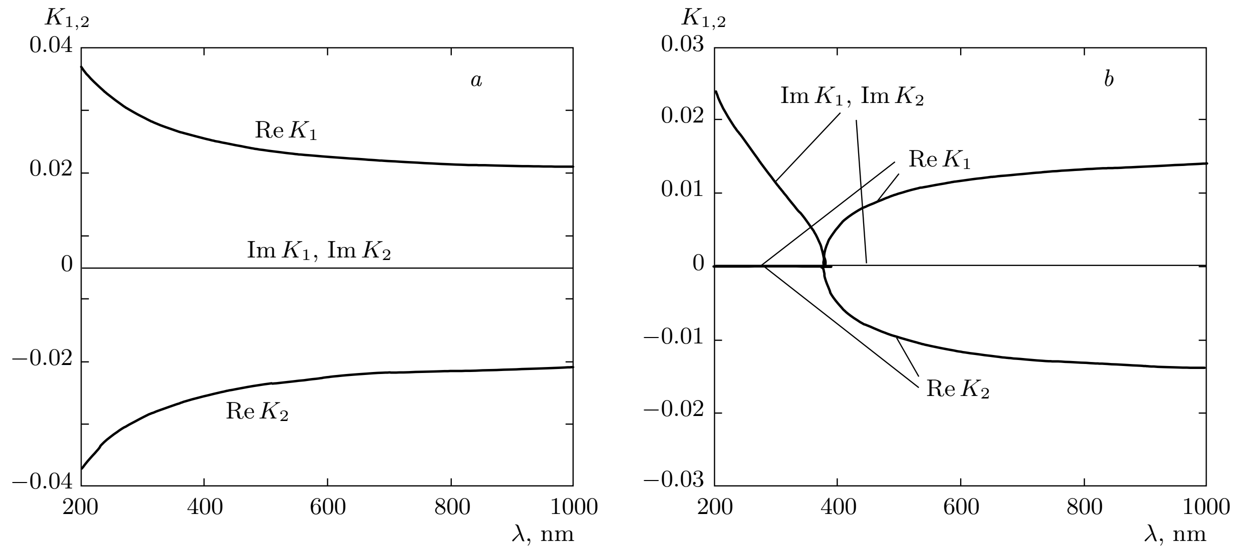

Fig. 3. The dependences of $K_{1,2}$ on the wavelength λ. The CLC parameters are (*a*) $\varepsilon_1 = -0.9$, $\varepsilon_2 = 0.9$, $\mu_1 = 0.9$, and $\mu_2 = -0.9$; (*b*) $\varepsilon_1 = -0.9$, $\varepsilon_2 = 0.9$, $\mu_1 = -0.9$, and $\mu_2 = 0.9$, and $p = 420$ nm

right-handed. The refractive indices of the isotropic layers are $n = 1.5$. Here and below, the case $n_0 = 1$ is considered, that is, we assume that the system is in the vacuum and, unless specified otherwise, it is assumed that the first sublayer of the system is isotropic. For the azimuth and the ellipticity of the second EP, we have $e_2 \approx -e_1$ and $\psi_2 \approx -\psi_1$. In Fig. 5, for comparison, we show the reflection spectra, the polarization plane rotation and the polarization ellipticity spectra, the spectra of the azimuth and the ellipticity of the first and second EPs for normal light incidence in the case of CLC layers with low dielectric and magnetic anisotropies. The comparison of the reflection spectra in Figs. 4 and 5 with the analogous spectra of the CLC single layer shows the following.

1) In the stack case, polarization sensitivity appears, in the case of normal light incidence, in spite of the polarization insensitivity of both the isotropic layer and the single CLC layer with chiral nihility. This sensitivity is conditioned by the difference of the EPs of these two layers, and due to this difference the EPs of the stacked structure differ from both the EPs of CLC layers and those of the isotropic layers.

2) In contrast to a single CLC layer with chiral nihility, this system has multiple PBGs, whereas for a single CLC layer with chiral nihility of the first type, as mentioned above, there is no PBG at all, while in the second case there is only one. Moreover, a stack with the CLC layers with chiral nihility of the second type also has a shortwave PBG in the spectrum region (15), as a single CLC layer with the chiral nihility of the same type. There are PBGs of two types: the PBGs independent of the incident light polarization and those dependent on the polarization. We note that the emergence of these two types of PBGs (those selective with respect to the incident light polarization and nonselective ones) has been observed for periodic chiral PCs of very different types [47–50]. The complicated zone structure is caused by light diffraction at the periodic chiral structure and that for the achiral ones, as well as by the coupling of waves of these two types.

As our numerical calculations show, in the case of a stack of CLC layers with the first chiral nihility type, for $n = 1.0$ (i. e., for the equidistant CLC layers, in the vacuum) there is no reflection at all ($R \equiv 0$) (as in the case of a single CLC layer with the corresponding chiral nihility type) for every polarization of the incident light and in all the optical spectral range, although the system is composed of isotropic layers and of CLC layers with significantly larger anisotropy. This peculiarities of the subject system can find wide applications, in particular, for creating nonreflecting coatings. Also, in this case, the system possesses gyrotropy (i. e., rotation of the polarization plane differs from zero and the ellipticity differs from linearity, for incident light with linear polarization.)

As our calculations show, the system EPs are nonorthogonal, but are quasi-circular and, for the odd sublayer number in the system, $e_2 = -e_1$ and $\psi_2 = -\psi_1$. If the sublayer number in the system is

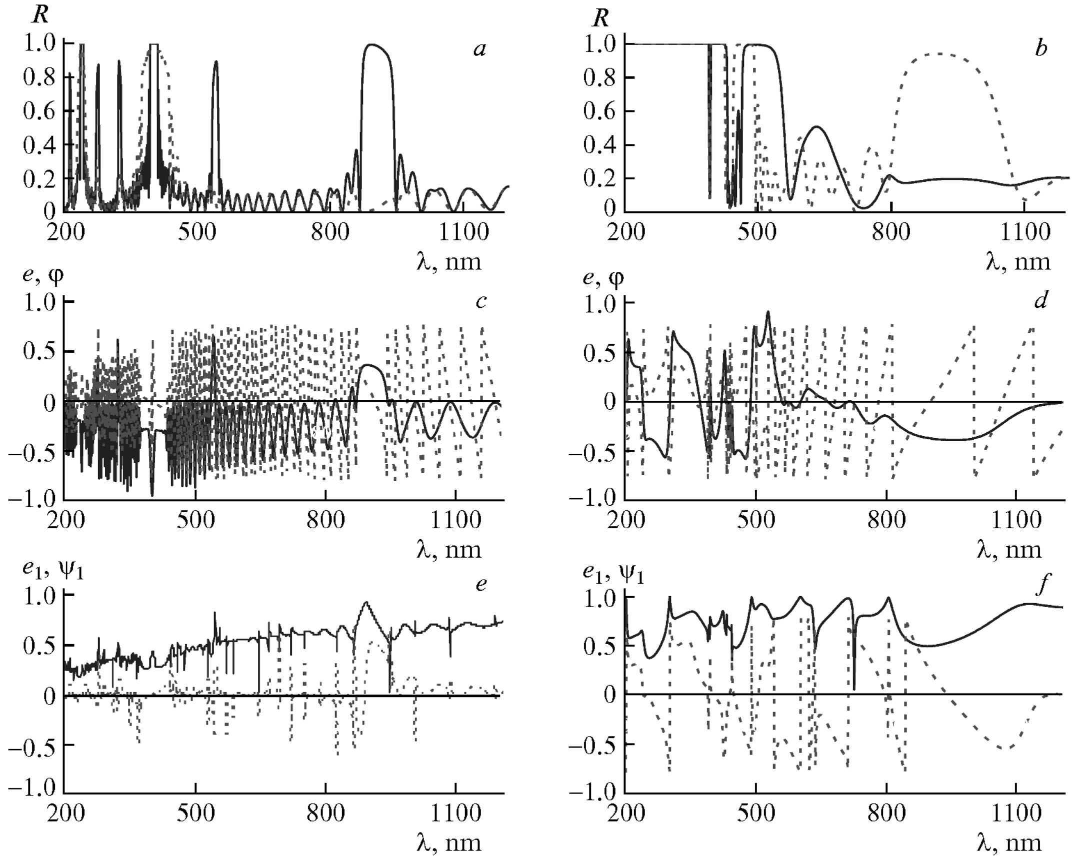

Fig. 4. (a and b) The reflection spectra, (c and d) the spectra of the polarization plane rotation (solid line) and polarization ellipticity (dashed line), and (e and f) the azimuth (dashed line) and the ellipticity (solid line) of the first EP in the cases (a, c, and e) a stack with CLC layers with chiral nihility of the first type, (b, d, and f) a stack with CLC layers with chiral nihility of the second type for normal light incidence. (a,b) incident light has the right (solid curve) and left (dashed curve) circular polarization, and (c,d) linear polarization along the x axis. The CLC layers helices are right handed, and $d = 2p$. The refractive index of the isotropic layers is $n = 1.5$ and their thicknesses are $d_1 = 200$ nm, $s = 50$ (a, c, and e) and $s = 10$ (b, d, and f). The other parameters are the same as in Fig. 3

even, e_2 can significantly differ from $-e_1$ and, accordingly, ψ_2 can significantly differ from $-\psi_1$. For $n = 1.0$, the EPs are orthogonal, $\chi_1\chi_2^* = -1$, for both even and odd sublayer numbers in the system. As our calculations show in the case $n = 1.0$, the system EPs are orthogonal elliptic polarizations for both types of nihilities. For the first type, the EP ellipticity monotonously increases with λ (in modulus), and for the second type, the EPs are orthogonal circular polarizations.

3.2. Influence of the thickness of CLC layers

We now pass to the investigation of the influence of the CLC layers thickness changes on the reflection spectra. As previously, we consider the case where the first sublayer is isotropic. In Fig. 6, the evolution of reflection spectra with changing the CLC layers thickness d is presented. The incident light has the left (left column) and right (right column) circular polarizations. The first row is for the stack with CLC layers with chiral nihility of the first type and the second row is for the stack with CLC layers with chiral nihility of the second type. Brighter regions present stronger reflection. As can be seen from Fig. 6, the frequency locations and frequency widths of the PBGs are functions of the CLC layers thicknesses. When the CLC layers thicknesses increase, the PBG quantity and their frequency widths change. The PBG frequency widths increase periodically; then they decrease, and all this occurs in significantly large intervals, especially in the longwave region. Also, it is seen from this figure that the bright lines are practically vertical in the longwave region for the left circularly polarized incident light if the stack

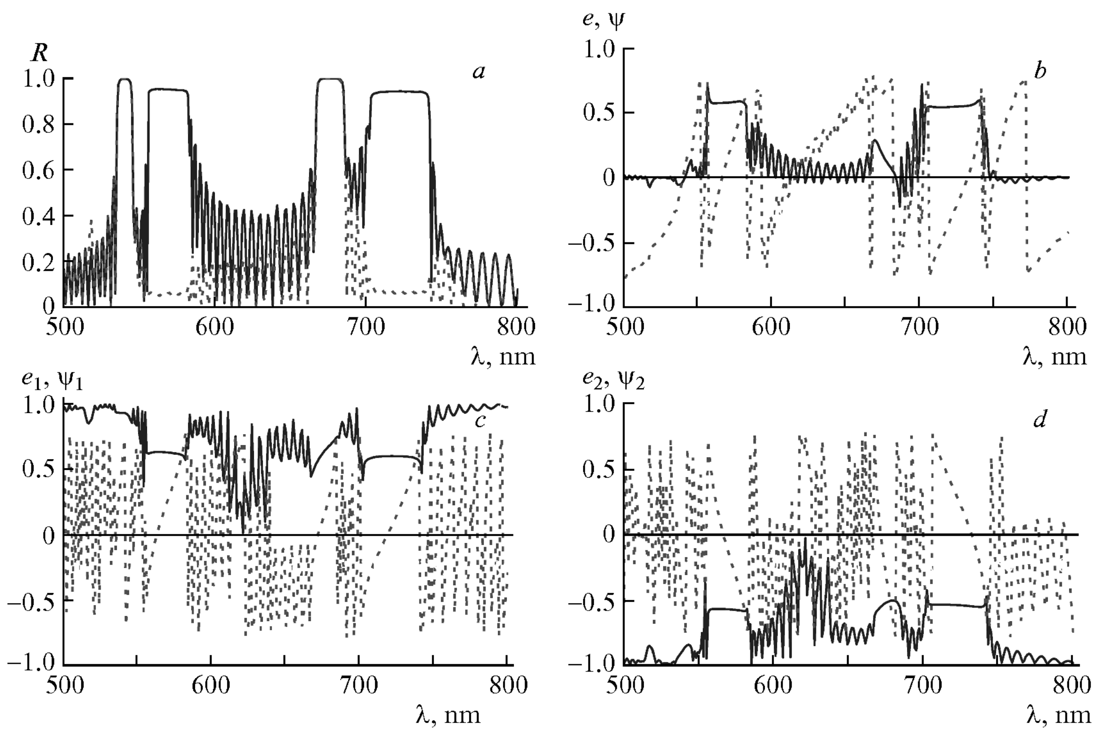

Fig. 5. (a) The reflection spectra, the spectra of (b) the polarization plane rotation and polarization ellipticity, (c and d) the azimuth and the ellipticity of the first and second EPs for low dielectric and magnetic anisotropies of CLC layers, $d = 1000$ nm. The refractive index of the isotropic layers is $n = 1.7$ and their thicknesses are $d_1 = 100$ nm. The other parameters are the same as in Fig. 2

with the CLC has chiral nihility of the first type and also for the right circularly polarized incident light and for the second type chiral nihility. This means that changing the thickness of CLC layers can either give rise PBGs with a very large frequency width or lead to their vanishing. Also, it is seen from the figure that the PBGs are not formed near the wavelength $\lambda = 600$ nm for any values of the CLC layer thicknesses. In the case of the stack with CLC layers with chiral nihility of the first type, the same holds near the wavelength $\lambda = 300$ nm. We note that these wavelengths satisfy the condition $nd_1 = i\lambda$ ($i = 1, 2, \ldots$).

If d increases, the slope of the PBG white stripes changes (with respect to the wavelength axis), i. e., an increase in d leads to a decrease or increase in the PBG maximum frequency width. In the case of a stack of CLC layers with chiral nihility of the second type, the frequency width of the shortwave PBG is practically unchanged if the thicknesses d increase (after their certain value). This shortwave PBG is observed in the stack of the CLC with the second-type chiral nihility and, as noted above, this PBG is also observed for a single CLC layer.

3.3. Influence of the CLC local dielectric anisotropy

The dielectric anisotropy $\Delta = (\varepsilon_1 - \varepsilon_2)/2$ is of the order of 0.5 or less for ordinary CLCs, but recently some artificial crystals (metamaterials) have been created with the dielectric anisotropy varying in a broad range. It seems that they can be used to fabricate CLC-like helical periodic media that have huge local anisotropy. Such media with a comparatively weaker anisotropy have been made long ago [51, 52]. On the other hand, there is considerable interest in the CLC doped with nanoparticles (either ferroelectric or ferromagnetic particles; see [53] and the references therein). The presence of these nanoparticles in the CLC structure leads to a significant increase in local (dielectric and magnetic) anisotropy, a significant change of the temperature of the phase transition from the isotropic phase to the liquid crystalline phase, significant change of the frequency width and frequency location of the

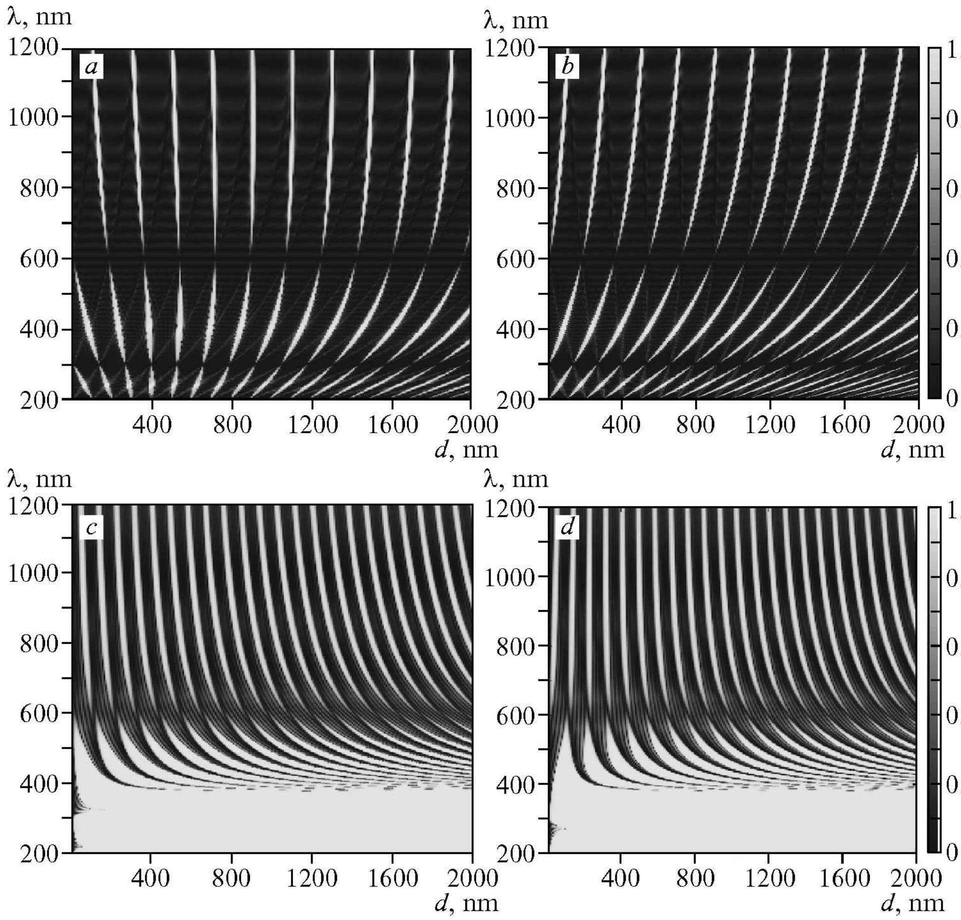

Fig. 6. Evolution of the reflection spectra as the CLC layers thicknesses d change. The incident light has (a and c) left and (b and d) right circular polarizations: (a and b) for a stack with CLC layers with chiral nihility of the first type and (c and d) for those of the second type. The other parameters are the same as in Fig. 3

PBG, a change of the CLC elasticity coefficients, and a significant increase in the tunability of CLCs, etc.

It follows from the foregoing that the investigation of the optical properties of stacks of CLC layers with chiral nihility and isotropic medium layers that have different values of local dielectric anisotropy, can be of great interest. Presenting the principal values of the local dielectric and magnetic tensors of the CLC sublayers in the form $\varepsilon_{1,2} = \mp(\varepsilon_0 - x)$ and $\mu_{1,2} = \pm(\mu_0 - x)$ for the first case (i. e., for $\varepsilon_m = \mu_m = 0$, $p \neq 0$, and $\varepsilon_1/\mu_1 = \varepsilon_2/\mu_2 < 0$), and $\varepsilon_{1,2} = \mp(\varepsilon_0 - x)$ and $\mu_{1,2} = \mp(\mu_0 - x)$ for the second case (i. e., for $\varepsilon_m = \mu_m = 0$, $p \neq 0$, and $\varepsilon_1/\mu_1 = \varepsilon_2/\mu_2 > 0$), we next investigate the influence of x on the reflection spectra.

In Fig. 7, we present the evolution of the reflection spectra with x (which characterizes the local dielectric and magnetic anisotropies). The incident light has the left (left column) and right (right column) circular polarizations. The first row pertains to the case of a stack with CLC layers with chiral nihility of the first type, and the second row, to that of the second type. As can be seen from the figure, these two cases differ from each other. Their common feature is that no PBG is formed near the values, $x = \varepsilon_0 = \mu_0$ ($\varepsilon_0 = \mu_0 = 2.5$), that is, at $\varepsilon_1 = \varepsilon_2 = \mu_1 = \mu_2 = 0$, which is natural. The number of PBGs and their frequency location and frequency width change as x changes. In the case of the stack with CLC layers with chiral nihility of the second type, if $|\varepsilon_0 - x|$ (or $|\mu_0 - x|$) increases, the frequency width of the PBGs that are not selective to the incident light polarization is significantly increased and, for larger values of this parameter, total reflection occurs in virtually the entire wavelength range. This is also natural because PBG is shortwave, with its longwave

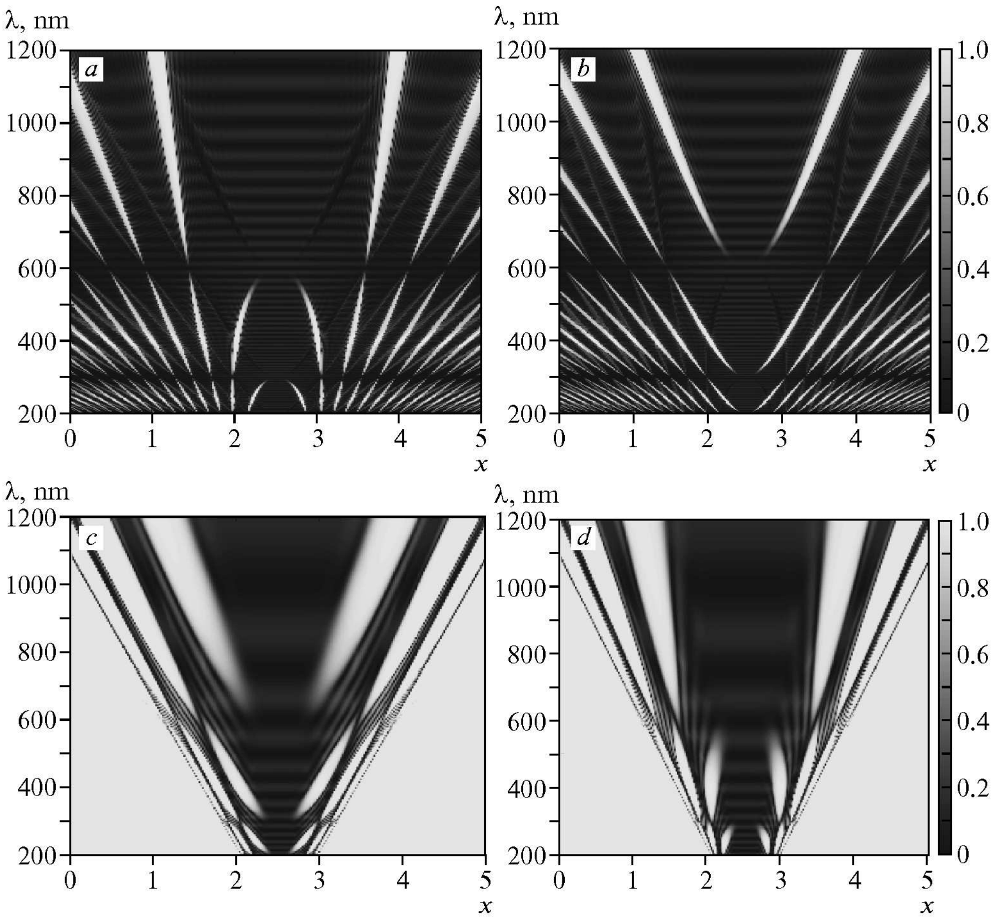

Fig. 7. Evolution of the reflection spectra as x (characterizing the anisotropy) changes: $x = \varepsilon_0 \pm \varepsilon_{1,2} = \mu_0 \mp \mu_{1,2}$ for a stack with CLC layers with the first type chiral nihility, and $x = \varepsilon_0 \mp \varepsilon_{1,2} = \mu_0 \pm \mu_{1,2}$ for a stack with CLC layers with the second type chiral nihility. The incident light has (a and c) left and (b and d) right circular polarizations: (a and b) for the stack with CLC layers with chiral nihility of the first type; and (c and d) is for those of the second type. $\varepsilon_0 = \mu_0 = 2.5$. The other parameters are the same as in Fig. 3

border shifted closer to the longwave region as $|\varepsilon_0 - x|$ (or $|\mu_0 - x|$) increases. In the case of the stack with CLC layers with chiral nihility of the first type, again, no PBG is formed near the wavelengths $\lambda = 600$ nm and $\lambda = 300$ nm, for all values of x.

Now, presenting the dielectric and magnetic tensor principal values for the CLC sublayers in the form $\varepsilon_{1,2} = \mp 1.25$ and $\mu_{1,2} = \pm y$ for the first case, and $\varepsilon_{1,2} = \mp 1.25$ and $\mu_{1,2} = \mp y$ for the second case, we investigate the influence of y on the reflection spectra. In Fig. 8, we present the evolution of the reflection spectra as y changes. The other parameters are the same as in Fig. 7. As can be seen from Fig. 8, the reflection of the system can also be tuned by changing y. Changes of y either lead to the vanishing of PBGs or give rise to PBGs with various values of frequency widths, polarization sensitively or insensitively, etc. That is, such a system can be used as a narrow-band (or a wide-band) filter or mirror.

3.4. Influence of the refractive indices of isotropic layers

We consider the influence of changes in the refractive indices of isotropic layers on the reflection spectra. In Fig. 9, evolution of the reflection spectra is presented, when the refraction index n of the isotropic layers is changed. The incident light has left (left column) and right (right column) circular polarizations. The first row is for the stack with the CLC layers with chiral nihility of the first type, and the second row is for that of the second type. As can be seen from the figure,

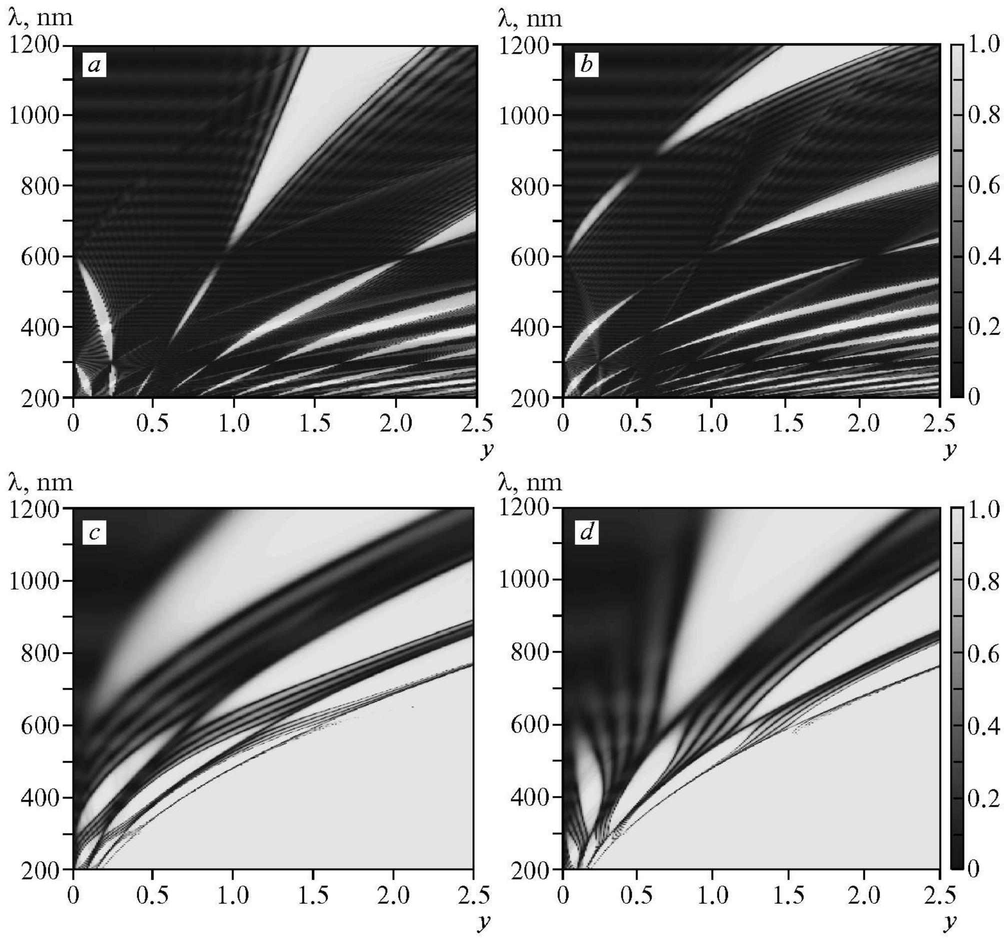

Fig. 8. Evolution of the reflection spectra as y changes: $\varepsilon_{1,2} = \mp 1.25$ and $y = \pm\mu_{1,2}$ for a stack with CLC layers with the first type chiral nihility, and $y = \mp\mu_{1,2}$ for a stack with CLC layers with the second type chiral nihility. The parameters and notations are the same as in Fig. 7

changing n also strongly influences the number of the PBGs, their frequency width, and frequency location. As n increases, the PBGs shift to the longer/shorter waves (depending on the incident light polarization and wavelength region), and the PBG frequency width oscillates and vanishes for certain values of n. As can be seen from Figs. 9c and 9d, in the case of the stack of CLC layers with the second type chiral nihility, the frequency width of the above shortwave PBG practically does not change if the index n increases, because the frequency width of this PBG is determined by the parameters of CLC sublayers.

3.4. Oblique incidence

We consider the oblique light incidence case. We do the numerical calculations as follows. First, we find the reflection and transmission matrices for each CLC sublayer. For this, we divide each CLC sublayer (with thickness d) into many thin layers with the thicknesses $l_1, l_2, l_3, \ldots, l_N$. If the maximum of these is sufficiently small, we can assume that each "subsublayer" is a linear birefringent plate, and the CLC sublayers with the thicknesses d can be regarded as stacks of parallel and very thin birefringent layers, and that the principal axis of each subsublayer is turned through the small angle $2\pi/N$ with respect to the preceding one. We find the reflection and transmission matrices of each CLC sublayer from the system of difference matrix equations (4), where $\hat{R}_j$, $\hat{T}_j$, $\hat{R}_{j-1}$, and $\hat{T}_{j-1}$ are the reflection and transmission matrices of the CLC sublayers with j and $(j-1)$ subsublayers, and $\hat{r}_j$ and $\hat{t}_j$ are the reflection and transmission matrices of the jth birefrin-

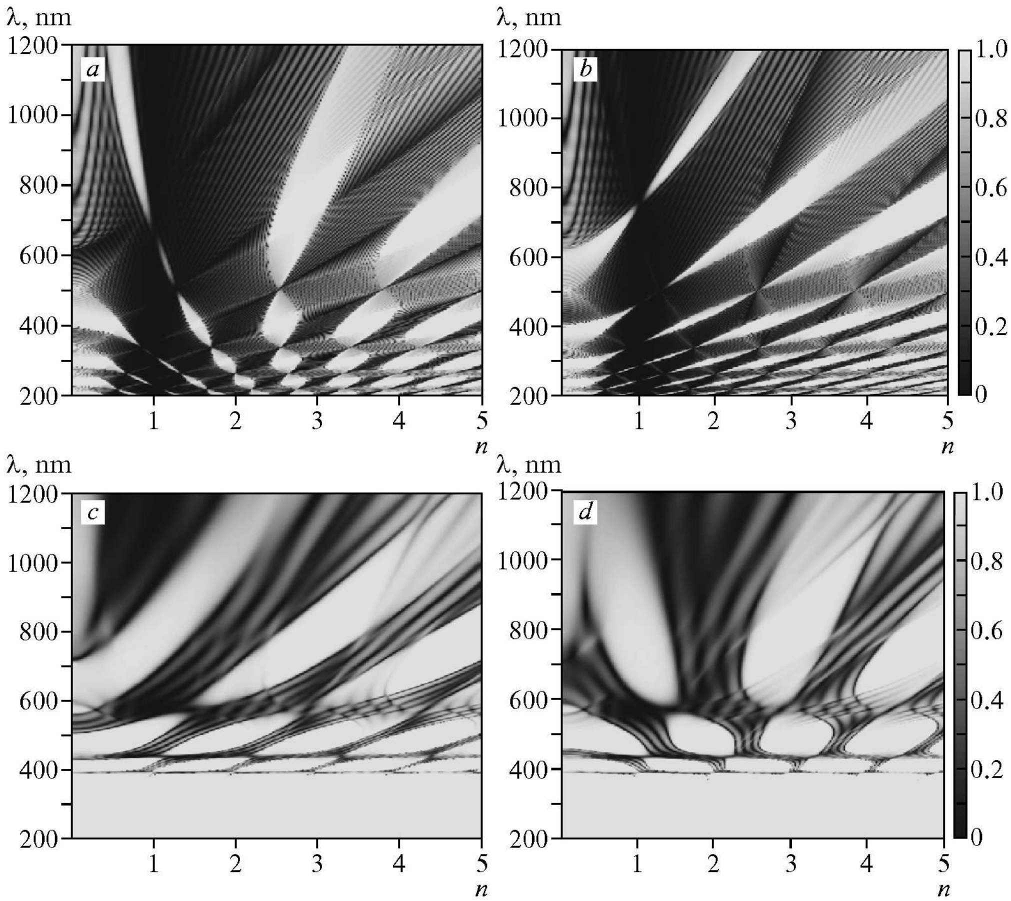

Fig. 9. Evolution of reflection spectra as the refractive index n of the isotropic layers changes. The incident light has (a and c) left and (b and d) right circular polarizations: (a and b) for a stack with CLC layers with chiral nihility of the first type; and (c and d) for those of the second type. The other parameters are the same as in Fig. 3

gent subsublayer. Then to calculate the reflection or transmission of the whole system, we again apply the system of difference matrix equations (4), but now $\hat{R}_j$, $\hat{T}_j$, $\hat{R}_{j-1}$, and $\hat{T}_{j-1}$ are the reflection and transmission matrices of the system with j and $(j-1)$ sublayers, and $\hat{r}_j$ and $\hat{t}_j$ are the reflection and transmission matrices of the jth sublayer (of the isotropic media or CLC). Thus, the problem is reduced to the calculation of the reflection and transmission matrices of a birefringent homogeneous layer. The analytic solution of this problem is well known (see, e. g., [54]). We pass to the analysis of the obtained results.

In Figs. 10a and 10b, the evolution of reflection spectra with the angle θ is presented. The incident light has right and left circular polarizations. The stack is composed of CLC layers with chiral nihility of the first type. As the incidence angle increases, the PBGs shift to short waves, but this shift is quite small or absent. Anyhow, this does not occur according to Bragg's condition

$$\lambda_B = \overline{n}\Lambda\cos\theta$$

(λ_B is the PBG central wavelength, $\overline{n}$ is the average refractive index of the medium, Λ is the spatial period, and θ is the incidence angle). This can be explained as follows. When the light incidence is oblique, for small oblique angles, the influence of Fresnel's reflection on the transmittance/reflection is comparatively small, but this influence significantly increases for larger angles. If there are no dielectric borders, the angle θ is simultaneously the incidence angle and the angle between the incident ray and the medium axis (the z axis in Fig. 1). If the dielectric borders are present, the incidence angle and the angle between the incident ray

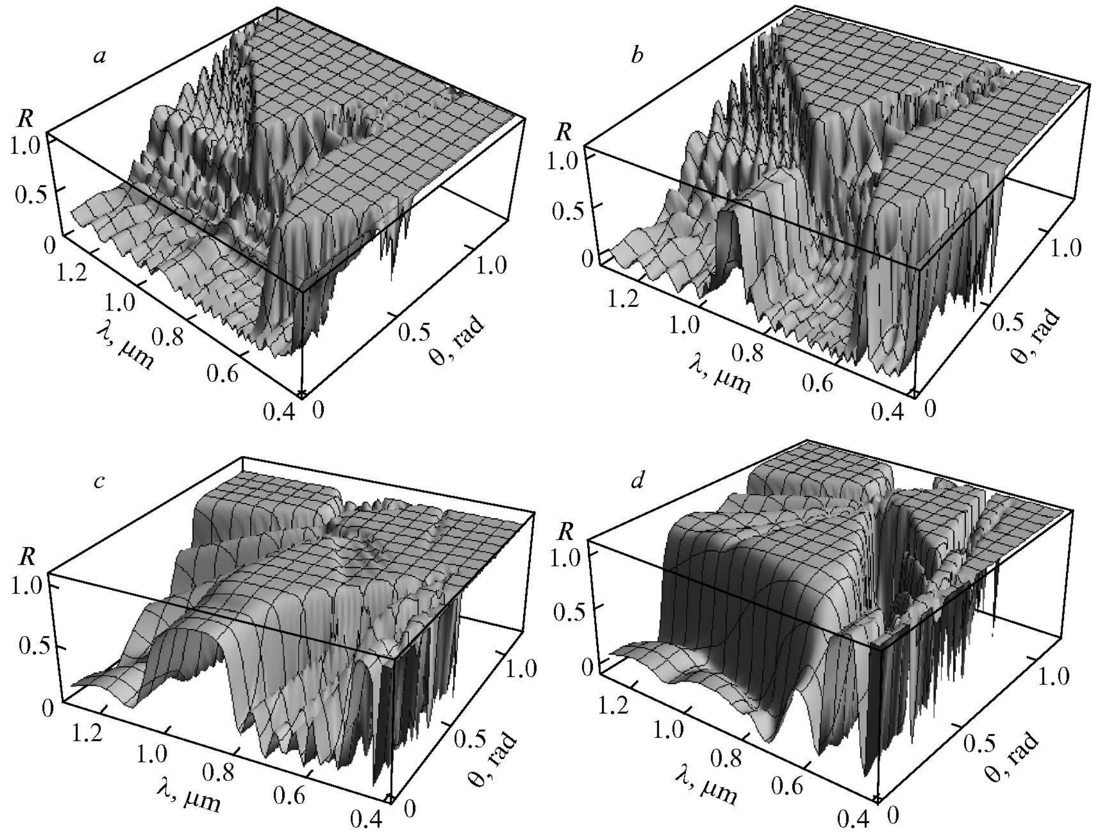

Fig. 10. Three-dimensional plots of the reflection coefficient R as a function of the wavelength λ and the incidence angle θ for a stack with CLC layers with chiral nihility of (a and b) the first and (c and d) the second type. The incident light has (a) left and (b) right circular polarizations. The other parameters are the same as in Fig. 3

and the medium axis differ from each other. According Snell's law, the angle θ must be replaced by the angle

$$\Theta = \arcsin\left(\frac{n_0}{\bar{n}}\sin\theta\right), \qquad (16)$$

where $n_0 = \sqrt{\varepsilon_0}$ is the refractive index of the medium bordering the system on both sides [55]. For Brewster's angle, the PBG width vanishes. The further increase in the incidence angle leads to an increase in the PBG frequency width, and this region becomes insensitive to the incident light polarization. We also note that as the incidence angle increases, new type PBGs occur in the short-wavelength region that are nonselective with respect to the incidence light polarization. Moreover, in contrast to the ordinary PBGs, the frequency width of these PBGs first increases, and then, beginning with a certain incidence angle, decreases. In contrast to usual crystals, at Brewster's angle, reflection vanishes only for the PBGs selective with respect to the incident light polarization.

Figures 10b and 10d show the same as Figs. 10a and 10b, i. e., the evolution of the spectra for the stack composed of the CLC layers with chiral nihility of the second type. In this case also, some complicated changes of the zone structure are observed as the incidence angle increases. Here, for larger angles, PBGs occur (with a significant frequency width) that are nonselective with respect to the incident light polarization.

4. CONCLUSION

Concluding, we note that we investigated the peculiarities of reflection spectra of a stack of CLC layers with chiral nihility and isotropic medium layers. These investigations give much information about new possibilities of applying chiral PCs in optics and photonics. Two types of CLCs with chiral nihilities were defined.

The main peculiarity of the reflection spectra of the usual single CLC layer is their polarization sensitivity (the reflection spectra are not identical for the two orthogonal circular polarizations of the incident wave). In the case of a single CLC layer with the second type chiral nihility, a new type of PBG appears that does not have polarization sensitivity. In the stack case, this new type of PBGs appears in any type of isotropic layers. Moreover, this system has multiple PBGs. This property of the subject system can find wide applications, in particular, in display manufacturing.

We have shown that changing the incidence angle and the system parameters (the thickness of CLC layers, their dielectric anisotropy, the isotropic layer thicknesses, their refractive indices, etc.), we can change the number of PBGs, their frequency width and frequency distance, and (in an essentially wide range) their character (whether they are selective or nonselective with respect to the incident light polarization), their gyrotropic properties, etc.

With the possibility of tuning of local parameters by changes in the external fields (electric, magnetic, mechanical, thermal, light, etc.), especially in the case where the system structure is soft, or the possibility of changing the internal structure of the system, the subject system has great prospects, in the sense of its applications in photonics.

In particular, the subject system can find application as a tunable optical filter or mirror, a tunable band asymmetric reflector, or as a system that allows obtaining 100 % polarized radiation from a nonpolarized light (without any loss), or as an antireflecting systems, etc.

The authors are grateful to the Referees for useful remarks. This work was partially supported by the Armenian National Science and Education Fund (ANSEF Grant No. Opt-3517).

REFERENCES

1. V. G. Veselago, Uspekhi Fiz. Nauk **92**, 517 (1976).
2. V. G. Veselago, Uspekhi Fiz. Nauk **172**, 1215 (2002).
3. K. Yu. Bliokh and Yu. P. Bliokh, Uspekhi Fiz. Nauk **174**, 439 (2004).
4. V. M. Agranovich and Yu. N. Gartstein, Uspekhi Fiz. Nauk **176**, 1051 (2006).
5. S. G. Rautian, Uspekhi Fiz. Nauk **178**, 1017 (2008).
6. D. R. Smith, W. J. Padilla, D. C. Vier et al., Phys. Rev. Lett. **84**, 4184 (2000).
7. R. A. Shelby, D. R. Smith, and S. Schultz, Science **292**, 77 (2001).
8. V. M. Shalaev, Nature Photonics **1**, 41 (2007).
9. S. H. Lee, C. M. Park, Y. M. Seo, and C. K. Kim, Phys. Rev. B **81**, 241102 (2010).
10. J. B. Pendry, Phys. Rev. Lett. **85**, 3966 (2000).
11. J. B. Pendry, D. Schurig, and D. R. Smith, Science **312**, 1780 (2006).
12. W. Cai, U. K. Chettiar, A. V. Kildishev, and V. M. Shalaev, Nature Photonics **1**, 224 (2007).
13. A. Alu and N. Engheta, Phys. Rev. E **72**, 016623 (2005).
14. F. J. Garcia de Abajo, G. Gomez-Santos, L. A. Blanco et al., Phys. Rev. Lett. **95**, 067403 (2005).
15. D. A. B. Miller, Opt. Express **14**, 12457 (2006).
16. U. Leonhardt, Science **312**, 1777 (2006).
17. N. I. Landy, S. Sajuyigbe, J. J. Mock et al., Phys. Rev. Lett. **100**, 207402 (2008).
18. K. Sakoda, *Optical Properties of Photonic Crystals*, Springer, Berlin (2001).
19. S. G. Johnson and J. Joannopoulos, *Photonic Crystals: The Road from Theory to Practice*, Kluwer, Boston (2002).
20. *Photonic Crystals and Light Localization in the 21st Century*, ed. by C. M. Soukoulis, NATO Science Series C, Vol. 563 (2001).
21. N. Y. Ha, Y. Ohtsuka, S. M. Jeong et al., Nature Mater. **7**, 43 (2008).
22. E. M. Nascimento, I. N. de Oliveira, and M. L. Lyra, J. Appl. Phys. **104**, 103511 (2008).
23. Z. He, Z. Ye, Q. Cui et al., Opt. Comm. **284**, 4022 (2011).
24. E. M. Nascimento, F. M. Zanetti, M. L. Lyra, and I. N. de Oliveira, Phys. Rev. E **81**, 031713 (2010).
25. N. Y. Ha, Y. Takanishi, K. Ishikawa, and H. Takezoe, Opt. Express **15**, 1024 (2007).
26. A. H. Gevorgyan, Phys. Rev. E **85**, 021704 (2012).
27. A. H. Gevorgyan, Opt. i Spectrosc. **113**, 162 (2012).
28. A. H. Gevorgyan, Mol. Cryst. Liq. Cryst. **559**, 76 (2012).
29. A. H. Gevorgyan, Izv. NAN Armenii, Fizika **47**, 407 (2012).
30. A. H. Gevorgyan, Izv. NAN Armenii, Fizika **48**, 111 (2013).
31. M. Z. Harutyunyan, A. H. Gevorgyan, and G. K. Matinyan, Opt. i Spectrosc. **114**, 654 (2013).

32. A. Lakhtakia, Int. J. Infrared and Millimeter Waves **23**, 813 (2002).

33. S. Tretyakov, I. Nefedov, A. Sihvola et al., J. Electromagn. Waves and Appl. **17**, 695 (2003).

34. C.-W. Qiu, N. Burokur, S. Zouhd, and L.-W. Li, J. Opt. Soc. Amer. A **25**, 55 (2008).

35. X. Cheng, H. Chen, B.-I. Wu, and J. A. Kong, IEEE Ant. Propag. Magaz. **51**, 79 (2009).

36. V. R. Tuz and C.-W. Qiu, Progr. Electromagn. Res. **103**, 139 (2010).

37. M. A. Baqir, A. A. Syed, and Q. A. Naqvi, Progr. Electromagn. Res. M **16**, 85 (2011).

38. A. H. Gevorgyan, Phys. Rev. E **83**, 011702 (2011).

39. A. A. Gevorgyan, Opt. i Spectrosc. **89**, 685 (2000).

40. R. M. A. Azzam and N. M. Bashara, *Ellipsometry and Polarized Light*, North-Holland, New York (1977).

41. L. B. Glebov, J. Lumeau, S. Mokhov et al., J. Opt. Soc. Amer. A **25**, 751 (2008).

42. S. Mokhov and B. Ya. Zeldovich, Proc. Roy. Soc. London A **464**, 3071 (2008).

43. E. I. Kats, Zh. Eksp. Teor. Fiz. **60**, 1172 (1971).

44. V. A. Belyakov, *Diffraction Optics of Complex-Structured Periodic Media*, Springer-Verlag, New York (1992).

45. J. W. Shelton and Y. R. Shen, Phys. Rev. A **5**, 1867 (1972).

46. A. H. Gevorgyan and M. S. Rafayelyan, J. Opt. **15**, 125103 (2013).

47. K. M. Flood and D. L. Jaggard, J. Opt. Soc. Amer. A **13**, 1395 (1996).

48. O. V. Ivanov and D. I. Sementsov, Pure Appl. Opt. **6**, 455 (1997).

49. K. Kim, H. Yoo, D.-H. Lee, and H. Lim, Waves Rand. Comp. Media **16**, 75 (2006).

50. V. R. Tuz, M. Y. Vidil, and S. L. Prosvirin, J. Opt. **12**, 095102 (2010).

51. K. Robbie, M. J. Brett, and A. Lakhtakia, Nature **384**, 616 (1996).

52. I. J. Hodgkinson, Q. H. Wu, B. Knight, A. Lakhtakia, and K. Robbie, Appl. Opt. **39**, 642 (2000).

53. S.-C. Jeng, S.-J. Hwang, Y.-H. Hung, and S.-C. Chen, Opt. Express **18**, 22572 (2010).

54. H. Wohler, M. Fritsch, G. Haas, and D. A. Mlynski, J. Opt. Soc. Amer. A **8**, 536 (1991).

55. A. H. Gevorgyan, Opt. i Spectrosc. **105**, 680 (2008).